Dissociative ionization of H_2 by fast protons: Three-body breakup and molecular-frame electron emission

C. Dimopoulou[1], R. Moshammer[1], D. Fischer[1], P.D. Fainstein[4], C. Höhr[1], A. Dorn[1],

J. R. Crespo López Urrutia[1], C.D. Schröter[1], H. Kollmus[2],

R. Mann[2], S. Hagmann[2,3], and J. Ullrich[1]

[1]Max-Planck-Institut für Kernphysik, Saupfercheckweg 1, 69117 Heidelberg, Germany

[2]Gesellschaft für Schwerionenforschung, Planckstr. 1, 64291 Darmstadt, Germany

[3]Institut für Kernphysik, August-Euler-Strasse 6, 60486 Frankfurt, Germany

[4]Centro Atómico Bariloche, Comisión Nacional de Energía Atómica, 8400 Bariloche, Argentina

PACS numbers: 34.50.Gb, 33.80.Eh

Abstract

Highly differential cross sections have been obtained for dissociative single ionization of H_2 by 6 MeV proton impact by measuring the momentum vectors of the electron and the H^+ fragment in coincidence. The investigation of the momentum balance of the fragments along the projectile beam provided detailed insight into the four-particle dynamics, even though the H atom is not detected. Within the axial recoil approximation, first molecular-frame angular distributions of emitted electrons have been determined for molecules oriented perpendicular to the projectile beam. They are compared to the predictions of a CDW-EIS calculation.

1. Introduction

The interaction of single photons or charged particles with simple molecules has attracted increasing attention. Molecular hydrogen has been the prototype system because it is the simplest diatomic molecule and because its vibrational motion is relatively fast, allowing to investigate the interplay between the electronic and the nuclear motion. For photon impact (for a review see [1] and references therein) interest was strongly fuelled by the advent of photoelectron-photoion coincidence techniques (see references in [2]) which are now able to provide fully differential data for electron emission. These techniques have enabled for the first time the determination of molecular-frame photoelectron angular distributions and, consequently, of the symmetries of the molecular states involved (see e.g. [3-7]), thus providing the ultimate testing ground for theory (see e.g. [8, 9]).

For ion impact the experimental situation is more complicated since one more particle has to be detected in the final state in order to obtain kinematically complete data. Fully differential cross sections (FDCS) for non-dissociative ionization of H_2 by fast ion impact have not been accessible until recently, where the obtained data revealed the role of molecular autoionization channels on the emission of very low-energy electrons [10]. Theoretically, ionization or fragmentation of (oriented) molecules by ion impact is more demanding as well and only a few predictions have been made up to now for fragmentation of even simple molecules.

Essentially two classes of experiments have been performed to investigate ion impact ionization and/or fragmentation of molecules: First, interference patterns are expected in the ionization spectra of diatomic molecules, resulting from the coherent electron emission from the two molecular centres, in analogy to Young's double-slit experiment [11, 12]. Although these effects appear even for random orientation of the molecular axis, they are more pronounced in the

molecular-frame electron angular distributions [9]. Recent experiments have shown the presence of interference effects in ion impact ionization of H_2 [13] and have triggered several calculations [14, 15] but part of the information was lost since the orientation of the molecule with respect to the incident beam could not be determined. Second, coincident ion momentum spectra have been measured providing detailed information on the kinetic energy released in the molecular fragmentation and the dynamics involved (see e.g. [16-21]). During the previous decades, dissociative ionization of H_2 has been extensively studied by measuring the energy distributions of the emitted H^+ and/or the cross sections of the different channels [22-24].

Here, we present highly differential data for dissociative single ionization of H_2 by 6 MeV proton impact, more precisely, for the ground state dissociation channel. To our knowledge, electron amission in all spatial directions has been explored for the first time in coincidence with the H^+ fragment. These data, along with the predictions of a CDW-EIS (continuum-distorted-wave eikonal-initial-state) calculation (for a review see [25]), enable us to investigate the four-body dynamics (e, H^+, H, projectile) and to provide molecular-frame electron angular distributions. The limitations of both, theory and experiment, will be discussed.

In general, as depicted in Fig. 1, two possible pathways can be distinguished in single ionization of H_2. First, a stable, possibly vibrationally excited H_2^+ ion remains after the removal of the electron (non-dissociative ionization: (1) in Fig. 1). Second, with a small probability of a few percent of all ionization events [22, 26], the molecule dissociates into an H^+ and an H atom (dissociative ionization). The latter happens either by the creation of an excited molecular ion which dissociates since all $(H_2^+)^*$ states are repulsive in the Franck-Condon region or by populating the vibrational continuum of the ground state of H_2^+, resulting into dissociation into an H^+ and an H(1*s*) (ground state dissociation: (2) in Fig. 1). Ionization plus excitation can be

separated from ground state dissociation using the fact that the kinetic energy of the H^+ from the former is typically of the order of a few eV, whereas from the latter it is in the sub-eV range [23, 27]. As an additional channel, double excitation of H_2 into autoionizing states is known to contribute within a few percent to the dissociative ionization [22, 24]. Here, we are concerned with ground state dissociation (channel (2) in Fig. 1) since in our experiment we have detected very low–energy (a few tenths of meV) H^+ ions. The contribution of the $Q_1{}^1\Sigma_u{}^+(1)$ doubly excited state of H_2 autoionizing into the vibrational continuum of the ground state of $H_2{}^+$ has been identified and discussed before [10].

2. Experiment

The experiment was performed at the Max-Planck-Institute in Heidelberg using a multi-electron recoil-ion momentum spectrometer ("Reaction Microscope" [2, 28]). A well-collimated (1 mm × 1 mm), pulsed (pulse length ≈ 1ns, repetition rate = 289 kHz) proton beam (beam current = 0.5 nA) with an energy of 6 MeV (projectile velocity: v_p = 15.5 a.u.) crosses a beam of H_2 provided by a gas jet. The randomly oriented target molecules are in the vibrational ground state, since they reach a temperature of less than 10 K after the supersonic expansion. The emitted electrons and the recoil ions were extracted into opposite directions along the projectile beam axis (longitudinal direction) by a weak (4.5 V/cm) electric field over 11 cm and were detected by two-dimensional position sensitive detectors. A uniform longitudinal magnetic field of 14 G confined the transverse motion of the electrons, such that all electrons with energy $E_e \leq 35$ eV were detected with the full solid angle. The momentum vectors of both, recoil ion ($H_2{}^+$ or H^+) and electron, are determined from their measured absolute times-of-flight and positions on the detectors, respectively.

For non-dissociative ionization, the H_2^+ ions were detected for transverse momenta $p_{r\perp} \leq$ 2.9 a.u., covering essentially the full solid angle. The transverse momentum transfer is calculated event by event from the transverse momenta of the electron and the H_2^+ ion $\mathbf{q}_\perp = (\mathbf{p}_{e\perp} + \mathbf{p}_{r\perp})$ with an estimated resolution of $\Delta q_\perp \leq 0.3$ a.u.. The main contribution to the ionization cross section comes from $q_\perp$ values lower than 1 a.u.. Longitudinally, the momentum balance is given by $q_{min} = p_{e\|} + p_{r\|}$. The small quantity $q_{min} = (I + E_e)/v_p \leq$ 0.1 a.u. is the minimum momentum transfer required to overcome the binding energy (I = 15.4 eV) of H_2 and eject an electron with energy $E_e \leq 35$ eV. Within q_{min} the longitudinal momenta of the electron and the H_2^+ essentially compensate each other i.e. $p_{e\|} \cong - p_{r\|}$. Therefore, the total momentum transfer given by $\mathbf{q} = \mathbf{q}_\perp + q_{min} \cdot \hat{u}_p$, where $\hat{u}_p$ is the unit vector along the initial projectile velocity, mainly points into the transverse direction.

For dissociative ionization, the H^+ ions were detected for transverse momenta $p_{r\perp} \leq 2.3$ a.u., corresponding to energies of less than 40 meV for $p_{r\|} = 0$, covering a solid angle of approximately 10 % for ground state dissociation. The achieved momentum resolution for the H^+ recoil ions was $\Delta p_{r\|} = 0.1$ a.u. in the longitudinal and $\Delta p_{r\perp} = 0.2$ a.u. in the transverse directions, respectively. For the electrons we estimated $\Delta p_{e\|} \cong 0.05$ a.u. and $\Delta p_{e\perp} = 0.1$ a.u.. For dissociative ionization, $\mathbf{q}_\perp$ is the sum of the transverse momenta of all the fragments $\mathbf{q}_\perp = \mathbf{p}_{e\perp} + \mathbf{p}_{r\perp} + \mathbf{p}_{n\perp}$ (hereafter we use the index r for the recoil H^+ ion and n for the neutral H atom) and cannot be determined event by event since the momentum vector of the H atom is not measured (kinematically non-complete experiment). However, we can expect that the values of the momentum transfer involved are similar to the ones in the non-dissociative ionization channel. The momentum balance in the longitudinal direction is given by $q_{min} = p_{e\|} + p_{r\|} + p_{n\|}$. Now, the small quantity $q_{min} = (\delta E + E_e)/v_p < 0.13$ a.u., where $\delta E = 18.1$ eV, is the minimum momentum

transfer required to overcome both the binding energy (15.4 eV) of H_2 and the dissociation energy (2.7 eV) of the H_2^+ ion and eject an electron with energy $E_e \leq 35$ eV.

3. Dynamics of the three-body breakup

Interesting questions concerning the dynamics of the three-particle fragmentation can be raised for dissociative single ionization. How is the momentum that was transferred by the projectile shared among the three target fragments? Is the electron emission independent from the nuclear fragmentation or not? Moreover, how does the electron emission depend on the orientation of the internuclear axis with respect to the momentum transfer? In general, our "non-complete" experiment does not provide sufficient information to answer these questions. Nevertheless, definite answers can be obtained by selecting specific conditions. For example, if one considers the momentum balance in the longitudinal direction only, it can be considerably simplified since $q_{min} < 0.13$ a.u. and thus can be safely neglected: $p_{e\|} + p_{r\|} + p_{n\|} = 0$. In addition, reasonable assumptions can be made for the nuclear fragments since they are obviously strongly correlated.

The longitudinal momentum distributions of the H^+ ions are shown in the upper row of Fig. 2, for slow ($E_e < 5$ eV) and fast ($E_e > 10$ eV) electrons, emitted into the forward or backward hemisphere, respectively, with respect to the incoming projectile direction. The longitudinal momentum distribution of the H_2^+ ion from the non-dissociative ionization is also shown for comparison: As expected, the momentum distributions of the H^+ ions are much broader, reflecting the energy released in the nuclear fragmentation. We observe that the maximum of the $p_{r\|}$ distribution of the H^+ ions is shifted in the direction opposite to the emitted electron, an effect which becomes more pronounced at high E_e. This suggests that the dissociative ionization proceeds through a two-step mechanism: In a first step, the electron is emitted as a result of the

interaction with the projectile. In a second step, the remaining H_2^+ ion, which is left in its vibrational continuum, dissociates. In this picture, the ionization process is independent from the dissociation. Since $p_{e\|} = -(p_{r\|} + p_{n\|})$, in the first step the centre of mass of the H_2^+ ion acquires a momentum $-p_{e\|}$ in order to compensate the momentum of the outgoing electron. In the second step, the H^+ and the H are emitted in opposite directions with equal momenta in the frame moving with the centre of mass of the H_2^+ ion, i.e. $(p_{e\|}/2 + p_{r\|}) = -(p_{e\|}/2 + p_{n\|})$. Then, the quantity $\tilde{p}_{r\|} = (p_{e\|}/2) + p_{r\|}$ corresponds to the H^+ momentum in the frame of the molecule. In the lower row of Fig. 2 we have plotted $\tilde{p}_{r\|}$ for slow and fast, forward as well as backward electron emission as in the upper row of Fig. 2. Obviously the $\tilde{p}_{r\|}$ distributions are peaking at zero, providing conclusive evidence that the shift observed in the upper row of Fig. 2 corresponds to the initial "kick" given to the centre of mass of the molecular ion by the outgoing electron.

If the suggested two-step mechanism is correct, $\tilde{p}_{r\|}$ should not depend on the electron emission characteristics. Indeed, as shown in Fig 3(a), the ratios of the $\tilde{p}_{r\|}$ distributions for electrons emitted in the forward and in the backward direction, for $E_e < 5$ eV as well as $E_e > 10$ eV, are constant within statistical errors. Also obvious is that electron emission in the forward direction exceeds the one in the backward direction by about a factor of 1.2 and 1.4 for $E_e < 5$ eV and $E_e > 10$ eV, respectively. This is due to a combination of pure kinematics, favouring in general the forward emission, and possibly of some remnants of the so-called post-collision interaction (PCI) at small perturbation $Z_p/v_p = 0.07$ in a.u. where Z_p is the projectile charge. At larger Z_p/v_p it is known that the electrons are "dragged" into the forward direction after the collision by the positive charge of the emerging projectile [29, 30].

In Fig 3(b) we have plotted the ratio of the $\tilde{p}_{r\|}$ distributions for fast and slow electrons. We see that the emission of fast electrons is slightly enhanced for large $\tilde{p}_{r\|}$. This might be attributed to the coupling between the electronic and the nuclear motion, which we have neglected so far. Since the momentum transfer is small (q_{min} < 0.13 a.u.), fast ($\tilde{p}_{r\|}$ > 2 a.u.) protons can only be ejected when the ground state dissociation occurs at very small internuclear distances within the Franck-Condon region (Fig. 1). Then, in turn, the emitted electrons might reach higher energies since they were initially more tightly bound in the molecule.

4. Molecular-frame electron emission

The molecular fragmentation process permits, under certain conditions, to determine indirectly the orientation of the molecular axis during the collision since the emission direction of the nuclear fragments might reflect the initial alignment of the molecule. When only one fragment is detected, in our case the H^+, the following conditions have to be fulfilled:

First, the momentum of the H^+ should be much larger than the momentum transfer and the momentum of the emitted electron. Then, the momentum of the H^+ mainly results from the kinetic energy released and its direction is determined by the orientation of the molecular axis at the instant of the fragmentation and not by the collision kinematics. This is in general not true in our experiment, since all the momenta involved have comparable magnitudes: q < 1 a.u., p_e < 1.6 a.u., p_r < 2.3 a.u.. However, since q_{min} is negligibly small, the direction of the H^+ is essentially unaffected by the kinematics in the special case when the H^+ is emitted perpendicular to the incoming projectile beam i.e. in the direction of $\mathbf{q} \approx \mathbf{q}_\perp$.

Second, the molecular dissociation should be fast in comparison to the molecular rotation, so that the direction of the detected H^+ really corresponds to the initial molecular orientation (axial recoil approximation [31]). This is valid for dissociation on the repulsive parts of all H_2^+ states as long as the energy of the emitted H^+ is higher than the rotational energy of the molecule [32, 33]. In our experiment most of the target molecules are estimated to reach the rotational ground state after the supersonic expansion, and therefore it was sufficient to consider H^+ ions with energies above 2 meV. (The experimental data showed no difference when we restricted to H^+ ion energies above 10 meV.)

Therefore, we have taken into account only events for which the H^+ was emitted

i) perpendicular to the projectile beam, more precisely under the condition $|\tilde{p}_{r||}| = |(p_{e||}/2) + p_{r||}| <$ 0.2 a.u., which corresponds to an H^+ emission angle between 80° and 100° and

ii) with energies above 2 meV, in order to fulfill the axial recoil approximation.

In Fig. 4 we present molecular-frame electron angular distributions for ground state dissociation of H_2 by ion impact. Plotted are doubly differential cross sections for electrons emitted into the plane defined by the momentum vectors of the incoming projectile, and the H^+ fragment as a function of the polar electron emission angle relative to the initial projectile direction, for E_e= 2.5 eV, 10 eV and 20 eV. With increasing E_e, the cross section slightly increases for electron emission opposite to the direction of the H^+ ion: this is due to the initial "kick" given to the centre of mass of the molecular ion by the outgoing electron in the transverse direction, similarly to what was said above for the longitudinal direction.

A theoretical CDW-EIS model [14, 34] has been developped in order to predict electron emission characteristics for non-dissociative ionization of H_2 ($H_2 \rightarrow H_2^+ + e^-$) as a function of the

orientation of the molecular axis. Briefly, the initial state of H_2 is approximated by a superposition of two hydrogenic orbitals centreed at each nucleus with a separation given by the equilibrium internuclear distance (R = 1.4 a.u.) and an effective charge of Z_{eff} = 1.19 to correctly reproduce the electronic binding energy. The resulting fully differential cross section for emission of an electron with momentum vector $\mathbf{k_e}$ is equal to the one for ionization of two "effective" H atoms multiplied by the oscillatory term $1+\cos\left[\left(\mathbf{k_e}-\mathbf{q}\right)\cdot\mathbf{R}\right]$. The latter represents the interference caused by the coherent emission from the two centres for a fixed orientation of the molecular axis **R**. Molecular effects beyond this and in particular the nuclear motion are not taken into account in this model.

A comparison between our experimental data and the predictions of the CDW-EIS calculation is possible within the frame of the following considerations: First, the electron emission characteristics for the ground state dissociation channel are assumed to be similar as for non-dissociative ionization since the kinetic energy released in the dissociation is very small (see Fig. 1). Second, while the theory considers only the orientation of the internuclear axis **R**, in the experiment we know in addition the direction of emission of the H^+. Thus, the theoretical predictions and the data can at least be compared in form, although their relative magnitude along 90° and 270°, respectively, might be different. Third, since the momentum transfer could not be determined experimentally, the theoretical FDCS have been integrated over $\mathbf{q}_\perp$.

The electron angular distributions calculated within the CDW-EIS in the plane defined by the direction of the incoming projectile and the molecular axis are shown in Fig. 4, as a function of the polar electron emission angle relative to the initial projectile direction, for E_e= 2.5 eV, 10 eV and 20 eV ("molecular calculation": solid lines). The cross sections for ionization of two "effective" H atoms, that is without the interference term, are also shown for comparison ("effective" atomic calculation: dashed lines). For these energies of the emitted electrons the

difference between “molecular” and “effective” atomic calculation is mainly visible in the absolute magnitude and is most pronounced at 90° and 270°. As explained in [34] the small structures appearing in the “molecular” calculation mainly in the forward and backward directions essentially result from the interference term. In Fig. 4 the experimental data are compared in shape to the theoretical calculations. For each E_e, the data have been normalised to the “molecular” CDW-EIS cross section in the region around 90°.

Within statistical errors the experimental data are found to be in good agreement with both calculations. In particular, the electron angular distribution becomes narrower along the perpendicular axis as E_e increases. According to the theory, interference effects become increasingly important as E_e increases or, equivalently, as the de Broglie wavelength of the emitted electron becomes comparable to the internuclear distance. In order to observe a full oscillation in the FDCS E_e should extend up to 270 eV. Thus, for the low electron energies considered here, interference effects are very small. In this respect, within the statistical errors, our experiment cannot provide evidence for them. Another question is whether they exist at all for dissociative ionization where we actually distinguish the two nuclear centres by knowing the emission direction of the H^+ ion. Since at present the only way to determine experimentally the orientation of the H_2 molecule is by dissociative ionization, this means that it might in principle be impossible to verify the theoretical predictions of interference patterns in molecular-frame electron emission.

5. Conclusions

We have studied dissociative single ionization of H_2 by 6 MeV proton impact by measuring the momentum vectors of the electron and the H^+ fragment in coincidence. By investigating the momentum balance of the fragments along the projectile beam we have verified experimentally that first the molecule is ionized and then, in a second step, it dissociates. Within the axial recoil approximation, we have measured for the first time molecular-frame electron angular distributions for molecules oriented perpendicular to the projectile beam. They are in good qualitative agreement with the predictions of a CDW-EIS calculation.

In the future, experiments are planned for (a) higher kinetic energy H^+ in order to determine molecular-frame electron spectra for all molecular orientations (i.e. not only for 90°) and (b) higher energies of the emitted electron in order to clarify whether the interference patterns are observable. Such highly differential measurements are by far not straightforward because the cross sections are very small. On the theoretical side, more refined models are obviously required in order to describe dissociative and non-dissociative ionization of oriented molecules taking into account the nuclear motion of the molecule.

Acknowledgements

We acknowledge support from the EU within the HITRAP Project (HPRI-CT-2001-50036) and from the DAAD-Fundación Antorchas cooperation program.

Figure captions

Fig. 1: Schematic potential curves for H_2 and H_2^+ illustrating the different single ionization channels (for detailed potential curves see [35, 36]).

Fig. 2 : Upper row: Longitudinal momentum distributions of the H^+ ions emitted in dissociative ionization of H_2 by 6 MeV proton impact for electron energies as indicated. Full symbols (squares/circles): the electrons are emitted in the forward direction ($p_{e\|} > 0$); open symbols (squares/circles): the electrons emitted in the backward direction ($p_{e\|} < 0$). Solid line in (a): Longitudinal momentum distribution of the H_2^+ ion from non-dissociative ionization of H_2 for $E_e \leq 35$ eV. Lower row: Longitudinal momentum distributions of the H^+ ions in the molecular frame i.e. as a function of $\tilde{p}_{r\|} = (p_{e\|}/2) + p_{r\|}$ (see text). Symbols as in the upper row.

Fig. 3: (a) Ratio of the $\tilde{p}_{r\|}$ distribution for forward electron emission to that for backward electron emission. Open circles: $E_e < 5$ eV; full circles: $E_e > 10$ eV**.**

(b) Ratio of the $\tilde{p}_{r\|}$ distribution for $E_e > 10$ eV (fast electrons) to that for $E_e < 5$ eV (slow electrons). For a few points, indicative error bars are given.

Fig. 4: Electron angular distributions for H_2 molecules oriented perpendicular to the incoming projectile beam and for $E_e = 2.5$ eV, 10 eV and 20 eV. The arrows indicate the emission direction of the detected H^+ fragment (see text). Solid lines: molecular CDW-EIS calculation; dashed lines: effective atomic CDW-EIS calculation. The cross sections are given in 10^{-20} cm^2/eV.

References

[1] Martín F 1999 *J. Phys. B: At. Mol. Opt. Phys.* **32** R197

[2] Ullrich J *et al* 2003 *Rep. Prog. Phys.* **66** 1463

[3] Lafosee A *et al* 2003 *J. Phys. B: At. Mol. Opt. Phys.* **36** 4683

[4] Eland J H D, Takahashi M and Hikosaka Y 2000 *Faraday Discuss.* **115** 119

[5] Ito K *et al* 2000 *J. Phys. B: At. Mol. Opt. Phys.* **33** 527

[6] Hikosaka Y and Eland J H D 2002 *Chem. Phys.* **277** 53

[7] Dörner R *et al* 1998 *Phys. Rev. Lett.* **81** 5776

[8] Dill D 1983 *J. Chem. Phys.* **65** 1130

[9] Walters M and Briggs J 1999 *J. Phys. B: At. Mol. Opt. Phys.* **32** 2487

[10] Dimopoulou C *et al* 2004 *Phys. Rev. Lett.* **93** 123203

[11] Cohen H D and Fano U 1966 *Phys. Rev.* **150** 30

[12] Kaplan I G and Markin A P 1969 *Sov. Phys.-Dokl.* **14** 36-9

[13] Stolterfoht N *et al* 2001 *Phys. Rev. Lett.* **87** 023201

[14] Galassi M E, Rivarola R D, Fainstein P D, Stolterfoht N 2002 *Phys. Rev.* A **66** 052705

[15] Stia C R *et al* 2003 *J. Phys. B: At. Mol. Opt. Phys.* **36** L257

[16] Ben-Izthak I, Ginther S G, Carnes K D 1993 *Phys. Rev.* A **47** 2827

[17] Ben-Izthak I, Ginther S G, KrishnamurthiV, Carnes K D 1995 *Phys. Rev.* A **51** 391

[18] Varghese S L *et al* 1989 *Nucl. Instrum. Methods* B **40**/**41** 266

[19] Adoui L *et al* 1999 *J. Phys. B: At. Mol. Opt. Phys.* **32** 631

[20] Tarisien M *et al* 2000 *J. Phys. B: At. Mol. Opt. Phys.* **33** L11

[21] Sobocinski P *et al 2002 J. Phys. B: At. Mol. Opt. Phys.* **35** 1353

[22] Ben-Izthak I *et al* 1996 *J. Phys. B: At. Mol. Opt. Phys.* **29** L21-L28

[23] Edwards A K, Wood R M, Beard A S and Ezell R L 1990 *Phys. Rev.* A **42** 1367

[24] Wood R M, Edwards A K and Steuer M F 1977 *Phys. Rev.* A **15** 1433

[25] Fainstein P D, Ponce V H, Rivarola R D 1991 *J. Phys. B: At. Mol. Opt. Phys.* **24** 3091

[26] Backx C, Wight G R and Van der Wiel M J 1976 *J. Phys. B: At. Mol. Opt. Phys.* **9** 315

[27] Wolff W *et al* 2002 *Phys. Rev.* A **65** 042710

[28] Moshammer R *et al* 1996 *Nucl. Instrum. Methods* B **108** 425

[29] Fainstein P D, Gulyás L, Martín F and Salin A 1996 *Phys. Rev.* A **53** 3243

[30] O' Rourke S F C, Moshammer R and Ullrich J 1997 *J. Phys.* B **30** 5281

[31] Zare R N 1967 *J. Chem. Phys.* **47** 204

[32] Dunn G H and Kieffer L J 1963 *Phys. Rev.* **132** 2109

[33] Wood R and Edwards A K 1997 *Accelerator-Based Atomic Physics Techniques and Applications* ed S M Shafroth and J C Austin (New York: AIP)

[34] Laurent G, Fainstein P D, Galassi M E, Rivarola R D, Adoui L and Cassimi A 2002 *J. Phys. B: At. Mol. Opt. Phys.* **35** L495

[35] Sharp T E 1971 *At. Data* **2** 119

[36] Guberman S L 1983 *J. Chem. Phys.* **78** 1404

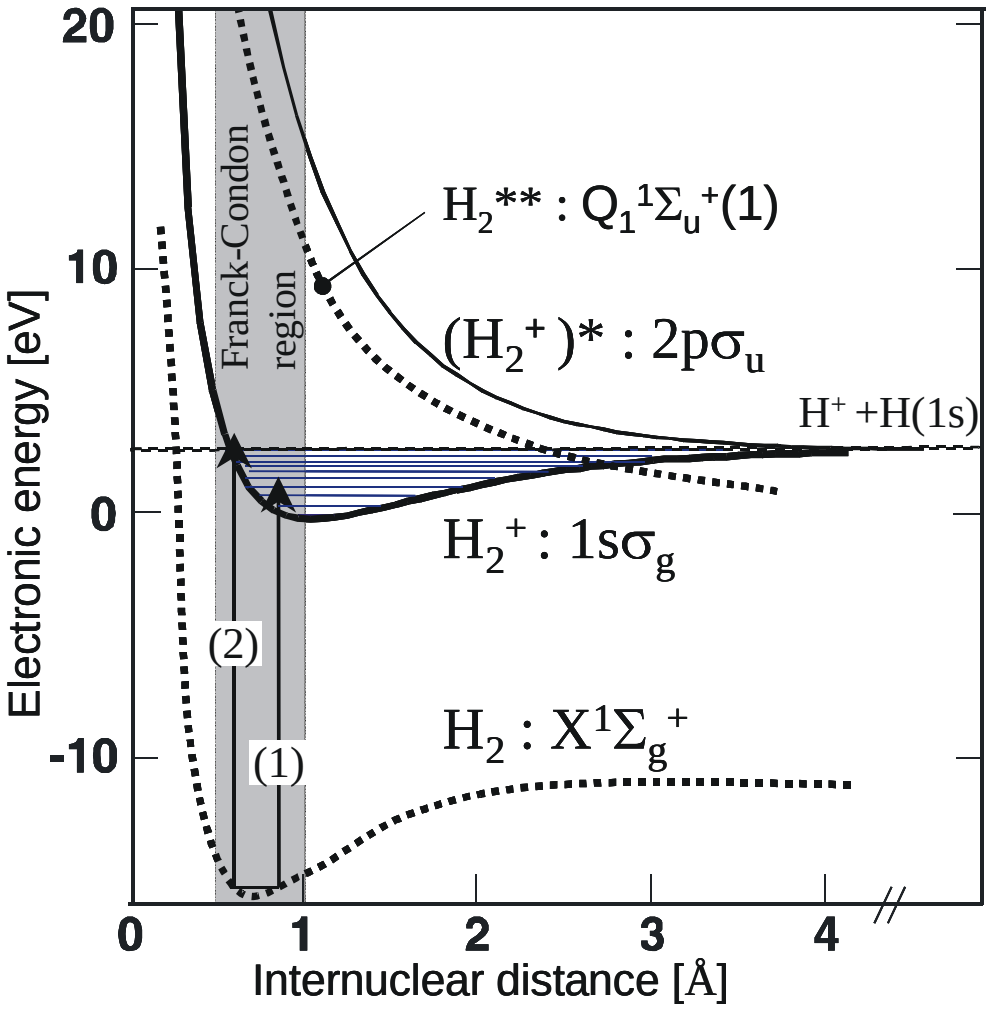
20
10
0
-10
Electronic energy [eV]
0
1
2
3
4
Internuclear distance [Å]
Franck-Condon region
H2** : Q1 1Σu+(1)
(H2+)* : 2pσu
H+ +H(1s)
H2+ : 1sσg
H2 : X1Σg+
(2)
(1)

Figure 1

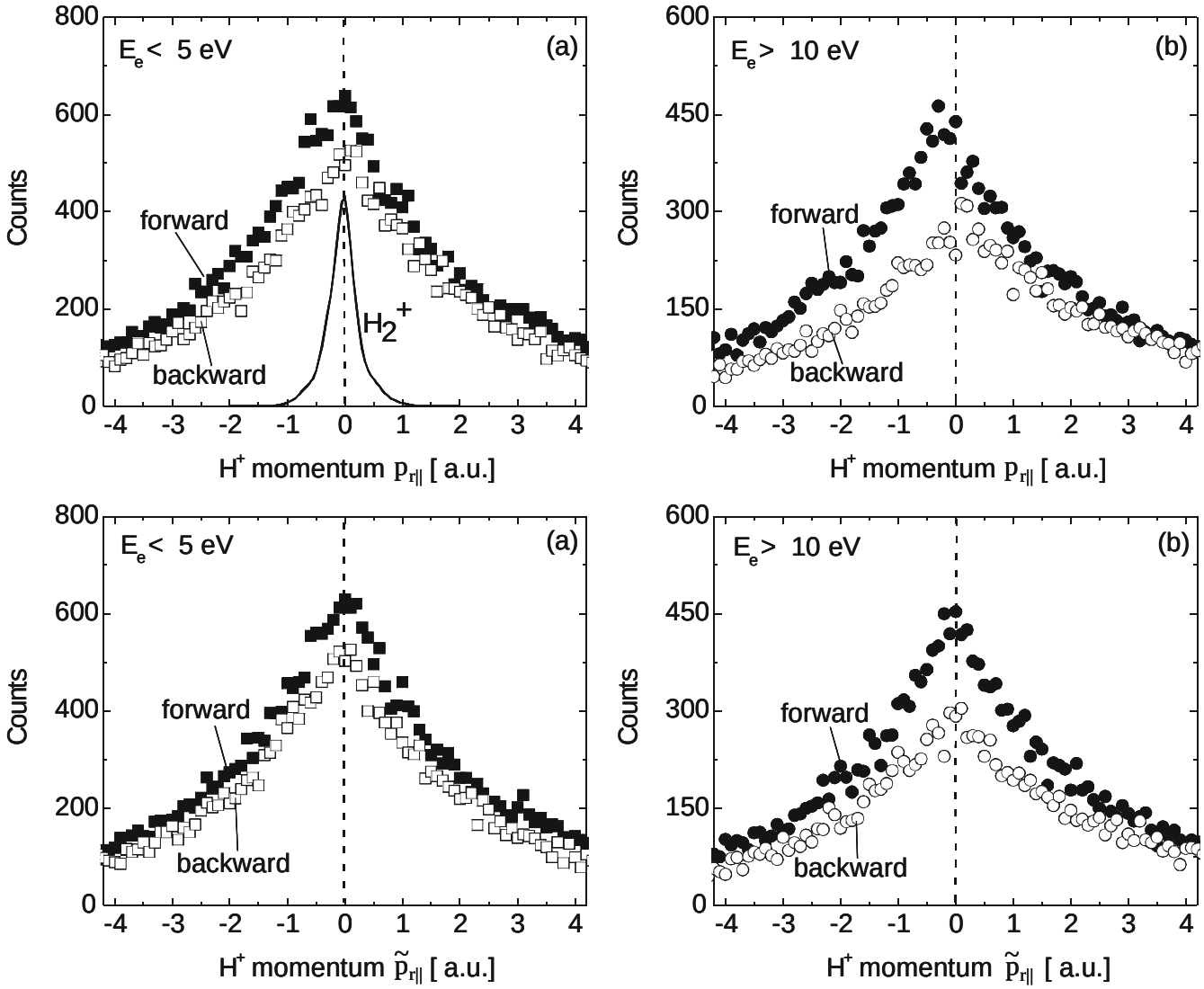
E_e < 5 eV
(a)
forward
backward
H2+
Counts
H+ momentum p_r|| [a.u.]
E_e > 10 eV
(b)
forward
backward
Counts
H+ momentum p_r|| [a.u.]
E_e < 5 eV
(a)
forward
backward
Counts
H+ momentum p̃_r|| [a.u.]
E_e > 10 eV
(b)
forward
backward
Counts
H+ momentum p̃_r|| [a.u.]

Figure 2

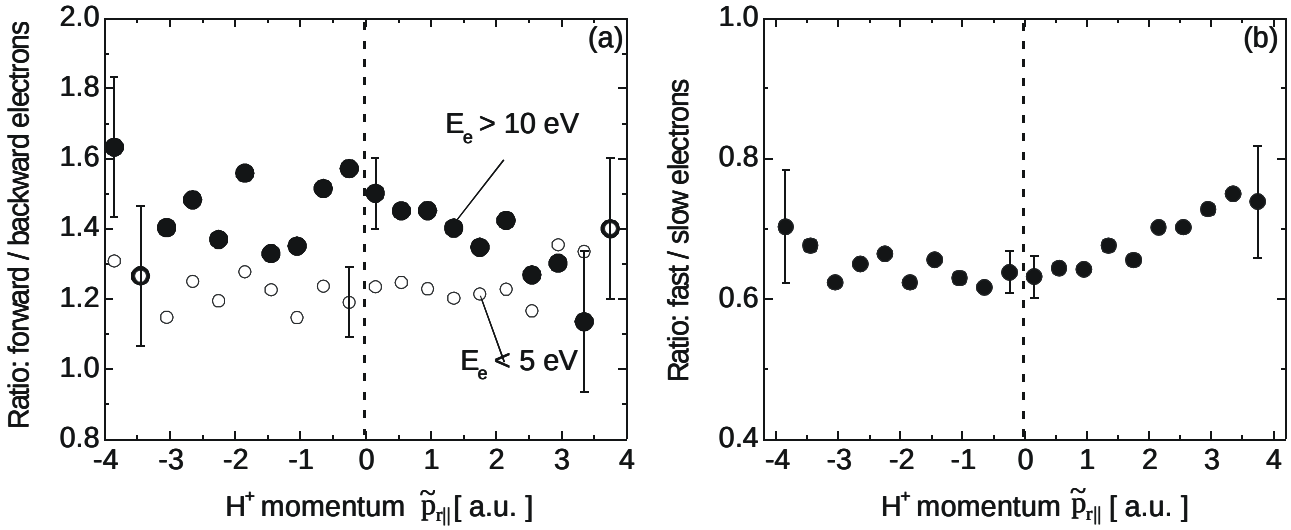

Figure 3

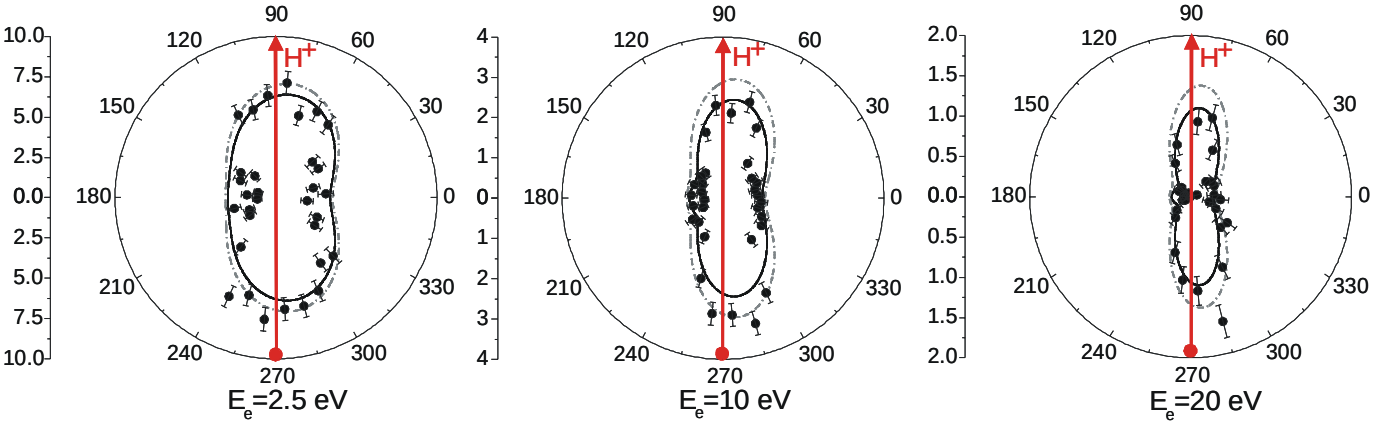

Figure 4